

Modern Feynman Diagrammatic One-Loop Calculations

Thomas Reiter¹, G. Cullen², N. Greiner³, A. Guffanti⁴, J.P. Guillet⁵,
G. Heinrich⁶, S. Karg⁷, N. Kauer⁸, T. Kleinschmidt⁶, M. Koch-Janusz¹,
G. Luisoni⁶, P. Mastrolia^{9,10,11}, G. Ossola¹², E. Pilon⁵, M. Rodgers⁶,
F. Tramontano¹¹, I. Wigmore²

¹ Nikhef, 1098 XG Amsterdam, The Netherlands,

² School of Physics and Astronomy, The University of Edinburgh, Edinburgh EH9 3JZ, UK,

³ Department of Physics, University of Illinois at Urbana-Champaign, Urbana IL, 61801, USA,

⁴ Physikalisches Institut, Albert-Ludwigs-Universität, 79104 Freiburg, Germany,

⁵ LAPTH, 74941 Annecy le Vieux Cedex, France,

⁶ IPPP, University of Durham, Durham DH1 3LE, UK,

⁷ Institut für Theoretische Teilchenphysik und Kosmologie, RWTH Aachen University, 52056 Aachen, Germany,

⁸ Department of Physics, Royal Holloway, University of London, Egham TW20 0EX, UK,

⁹ Centro Studi e Ricerche “E. Fermi”, 00184 Rome, Italy,

¹⁰ Dipartimento di Fisica, Università di Salerno, 84084 Fisciano (SA), Italy,

¹¹ Theory Group, Physics Department, CERN, 1211 Geneva 23, Switzerland,

¹² Physics Department, New York City College of Technology, City University Of New York, Brooklyn NY 11201, USA

November 6, 2018

Abstract

In this talk we present techniques for calculating one-loop amplitudes for multi-leg processes using Feynman diagrammatic methods in a semi-algebraic context. Our approach combines the advantages of the different methods allowing for a fast evaluation of the amplitude while monitoring the numerical stability of the calculation. In phase space regions close to singular kinematics we use a method avoiding spurious Gram determinants in the calculation. As an applica-

tion of our approach we report on the status of the calculation of the amplitude for the process $pp \rightarrow b\bar{b}b\bar{b} + X$.

1 Introduction

The experimental precision expected to be reached at the LHC demands cross-section calculations to move from the leading order approximation (LO) to the next-to-leading order (NLO) for many processes with three, four or even more particles in the final state. The complexity introduced by both the real and virtual corrections can only be overcome using automatised tools in the construction of programs for the numerical evaluation of their matrix elements.

An important step towards the automatisation of NLO calculations was the formulation of local subtraction terms which render real and virtual corrections independently infrared finite. The two most commonly used subtractions at the one-loop level are the dipole formalism [1, 2] and the FKS subtraction method [3, 4], both of which have led to several packages for their automated implementation [5–12]. As one of their advantages, subtraction methods offer a well-defined way of separating the different parts of a one-loop calculation. Inspired by this separation, at the Les Houches workshop a standard interface between Monte Carlo tools, computing the Born level, the real corrections and the subtraction terms, and one-loop programs which only need to provide the virtual corrections has been proposed [13].

The persistent efforts spent on the improvement of the methods for the calculation of one-loop amplitudes have recently induced a rapid growth in the number of NLO predictions for the LHC. The most recent results with four and more final state particles at the LHC are the corrections to $pp \rightarrow b\bar{b}t\bar{t} + X$ [14–16], $pp \rightarrow V + 3j$ [17–19], $pp \rightarrow W^\pm + 4j$ [20], $pp \rightarrow W^+W^+jj$ [21] and the $q\bar{q}$ initiated channel of $pp \rightarrow b\bar{b}b\bar{b} + X$ [22]. However, many Standard Model processes of similar complexity which are relevant for the discovery and/or the measurement of the properties of the Higgs boson or new particles from extensions beyond the Standard Model (BSM) are not yet available at NLO [23]. Moreover, once new particles are found at the LHC, their detailed study will require NLO studies in BSM models. We have therefore developed and implemented methods for the automated evaluation of one-loop Feynman diagrams, which we describe in Section 2. In Section 3, we present applications of our method, one of which is the calculation of the gluon induced channel of the process $pp \rightarrow b\bar{b}b\bar{b} + X$.

2 Method

2.1 A Numerator Representation for Feynman Diagrams

Our method for the calculation of one-loop matrix elements is based on the evaluation of Feynman diagrams. A one-loop diagram can be written as

$$\mathcal{D} = \int \frac{d^n q}{i\pi^{n/2}} \frac{\mathcal{N}(q, \varepsilon)}{D_1 \cdots D_N}, \quad (1)$$

where $D_i = [(q + r_i)^2 - m_i^2 + i\delta]$ and the integration momentum can be split into its projection \hat{q}^μ on the physical Minkowski space and an orthogonal component \tilde{q} . Instead of a single diagram, \mathcal{D} can also refer to a group of diagrams sharing the same set of denominators. All quantities are defined such that the following equations hold:

$$g^{\mu\nu} = \hat{g}^{\mu\nu} + \tilde{g}^{\mu\nu}, \quad \hat{g}_\mu^\mu = 4, \quad \tilde{g}_\nu^\mu = -2\varepsilon, \quad (2a)$$

$$\hat{g}_\rho^\mu \hat{g}^{\rho\nu} = \hat{g}^{\mu\nu}, \quad \tilde{g}_\rho^\mu \tilde{g}^{\rho\nu} = \tilde{g}^{\mu\nu}, \quad \hat{g}_\rho^\mu \tilde{g}^{\rho\nu} = 0, \quad (2b)$$

$$\hat{q}^\mu = \hat{g}_\nu^\mu q^\nu, \quad \tilde{q}^\mu = \tilde{g}_\nu^\mu q^\nu, \quad q^2 = \hat{q}^2 - \mu^2. \quad (2c)$$

The numerator of the integral can then be expressed in terms of the quantities (\hat{q}, μ^2) as

$$\mathcal{N}(q, \varepsilon) = \mathcal{N}_0(\hat{q}, \mu^2) + \varepsilon \mathcal{N}_1(\hat{q}, \mu^2) + \varepsilon^2 \mathcal{N}_2(\hat{q}, \mu^2) + \mathcal{O}(\varepsilon^3). \quad (3)$$

The functions \mathcal{N}_1 and \mathcal{N}_2 are relevant in regularisation schemes, where internal gauge bosons are kept in n dimensions ($n - 2$ polarisations), such as the 't Hooft-Veltman scheme or naïve dimensional regularisation. The terms originating from \mathcal{N}_2 are of purely infrared origin and therefore have to cancel out, as shown in [14]. These terms can serve as an additional check on the amplitude or simply be skipped in the computation. In the following discussion there is no need to distinguish between the individual functions $\mathcal{N}_i(\hat{q}, \mu^2)$, as we can simply consider the calculation of a diagram as separate calculations of the three terms in $\mathcal{D} = \mathcal{D}_0 + \varepsilon \mathcal{D}_1 + \varepsilon^2 \mathcal{D}_2$. We refer to these functions collectively as $\mathcal{N}(\hat{q}, \mu^2)$.

For the algebraic construction of $\mathcal{N}(\hat{q}, \mu^2)$ from the underlying Feynman rules we use QGraf [24] for generating the diagrams and Form [25] for their algebraic simplification. Since we work with helicity projections of amplitudes, we have devised a Form library for the manipulation of expressions containing helicity spinors [26] which is publicly available¹.

In amplitudes containing external partons, the matrix element and therefore each diagram is a vector in colour space $\mathcal{D} = \sum_c \mathcal{D}^c |c\rangle$. We avoid working with the vector components \mathcal{D}^c by contracting each diagram with the tree level amplitude, and working

¹<http://sourceforge.net/projects/spinney-form/>

with the corresponding numerator functions

$$\mathcal{N}_i^{(\text{QCD})}(\hat{q}, \mu^2) = \sum_{c, c'} \left(\mathcal{A}_{\text{Born}}^{c'} \right)^\dagger \mathcal{N}_i^c(\hat{q}, \mu^2) \langle c' | c \rangle. \quad (4)$$

This step is important to avoid a proliferation of numerical tensor reductions. In fact, one cannot avoid working with the components \mathcal{D}^c for processes where the Born level vanishes and at the first non-vanishing order one has to calculate the square of the NLO matrix element².

2.2 Tensor Reduction at the Integrand Level

Complete reducibility of one-loop diagrams to scalar integrals implies that the q -dependence of the numerator can be expressed in terms of the denominators D_i [27–31]:

$$\begin{aligned} \mathcal{N}(\hat{q}, \mu^2) = & \sum_{j_1 < \dots < j_{N-1}} a_{j_1 \dots j_{N-1}}(q) D_{j_1} \cdots D_{j_{N-1}} \\ & + \sum_{j_1 < \dots < j_{N-2}} b_{j_1 \dots j_{N-2}}(q) D_{j_1} \cdots D_{j_{N-2}} \\ & + \sum_{j_1 < \dots < j_{N-3}} c_{j_1 \dots j_{N-3}}(q) D_{j_1} \cdots D_{j_{N-3}} \\ & + \sum_{j_1 < \dots < j_{N-4}} d_{j_1 \dots j_{N-4}}(q) D_{j_1} \cdots D_{j_{N-4}} \\ & + \sum_{j_1 < \dots < j_{N-5}} d_{j_1 \dots j_{N-5}}(q) D_{j_1} \cdots D_{j_{N-5}}. \quad (5) \end{aligned}$$

The calculation of a one-loop diagram therefore amounts to the extraction of the coefficients, which are the residues of the integrand at the cuts $D_{j_1} = \dots = D_{j_r} = 0$. A suitable parametrisation of the coefficients and a fast implementation of the method in terms of a **Fortran 90** library **SAMURAI**³ is described in [32].

The decomposition given in Equation (5) works with n -dimensional rather than four-dimensional propagators $\hat{D}_i = [(\hat{q} + r_i)^2 - m_i^2]$ and keeps the dependence on μ^2 in the numerator. This improvement over the original OPP method [27, 28] allows the determination of the amplitude including both the cut-constructible and the rational part. The **SAMURAI** implementation also includes several reconstruction tests which provide a measure for the quality of the numerical result for a given diagram. This information can be used to dynamically switch to an alternative reduction method when

²We keep the name *NLO* for the one-loop order even if the Born level vanishes and the one-loop matrix element formally becomes the LO.

³<https://samurai.web.cern.ch/samurai/>

the precision of the reconstruction is not sufficient. Typically, unitarity based reduction methods fail in the neighbourhood of kinematical points with vanishing Gram determinants. Traditionally, implementations of unitarity methods go to higher precision when such a case is detected. The following two sections introduce a method which avoids the use of higher precision implementations.

2.3 Improved Algebraic/Numerical Tensor Reduction

The shortcomings of tensor reduction methods in the neighbourhood of vanishing Gram determinants can be cured either by expanding tensor coefficients about limits of vanishing Gram determinants [33] or by extending the integral basis by integrals which are non-scalar but which have fast and stable implementations [34–36]. The latter approach has been followed in implementing the `Fortran 95` library `Golem95` [37]⁴, which in its current version can be used for the reduction of tensor integrals with up to six external legs for massive and massless loop-propagators. For some $R \leq N$, the numerator structure of a Feynman diagram in a gauge theory can always be written as

$$\mathcal{D}_i = \int \frac{d^n q}{i\pi^{n/2}} \frac{\sum_{r=0}^R C_{\mu_1 \dots \mu_r}^{(r)} q^{\mu_1} \dots q^{\mu_r}}{D_1 \dots D_N} = \sum_{r=0}^R C_{\mu_1 \dots \mu_r}^{(r)} I_N^{n, \mu_1 \dots \mu_r}, \quad (6)$$

where the tensor integrals have the decomposition

$$\begin{aligned} I_N^{n, \mu_1 \dots \mu_r} = & \sum_{j_1 \dots j_r} [r_{j_1} \dots r_{j_r}]^{\mu_1 \dots \mu_r} A_{j_1 \dots j_r}^{N, r} + \sum_{j_1 \dots j_{r-2}} [g^{\cdot\cdot} r_{j_1} \dots r_{j_{r-2}}]^{\mu_1 \dots \mu_r} B_{j_1 \dots j_{r-2}}^{N, r} \\ & + \sum_{j_1 \dots j_{r-4}} [g^{\cdot\cdot} g^{\cdot\cdot} r_{j_1} \dots r_{j_{r-4}}]^{\mu_1 \dots \mu_r} C_{j_1 \dots j_{r-4}}^{N, r}. \end{aligned} \quad (7)$$

The coefficient functions $A^{N, r}$, $B^{N, r}$ and $C^{N, r}$ are implemented in the `Golem95` library, which apart from these tensor coefficients, also provides all the scalar integrals, both finite and divergent ones⁵, involving massless and massive particles with real masses. An extension of the library which, amongst other improvements, allows for complex masses will be released soon.

2.4 Tensorial Reconstruction at the Integrand Level

In Equations (5) and (6) we introduced two different decompositions of the numerator function $\mathcal{N}(\hat{q}, \mu^2)$, which can be rewritten as

$$\mathcal{N}(\hat{q}, \mu^2) = \sum_{\alpha=0}^{\lfloor R/2 \rfloor} (\mu^2)^\alpha \sum_{r=0}^{R-2\alpha} \hat{C}_{\mu_1 \dots \mu_r}^{(r, \alpha)} \hat{q}^{\mu_1} \dots \hat{q}^{\mu_r} \quad (8)$$

⁴<http://lapth.in2p3.fr/Golem/golem95.html>

⁵regulated dimensionally

It turns out that a method for the numerical reconstruction of the tensor coefficients $\hat{C}^{(r,\alpha)}$ can be constructed by means of extracting the coefficients of a multivariate polynomial in the variables $(\hat{q}^0, \dots, \hat{q}^3, \mu^2)$. As explained in Section 2.2, a numerical implementation of $\mathcal{N}(\hat{q}, \mu^2)$ is sufficient as input for such a reconstruction, which is described in detail in [38]. For nearly all relevant cases tensorial reconstruction (8) requires fewer samplings of the numerator function than reduction at the integrand level (5). An improvement of the SAMURAI algorithm can therefore be achieved by passing a numerator function to the tensor reduction which has been obtained from the original numerator by tensorial reconstruction. Another possibility is to combine SAMURAI and Golem95 as shown in Figure 1.

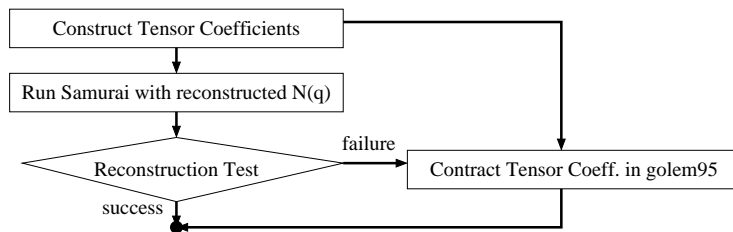


Figure 1: Possible ways of using SAMURAI and Golem95 together with tensorial reconstruction. On the left branch SAMURAI is called with the numerator reconstructed according to Eq. (8), which can speed up the calculation. If the consistency check in SAMURAI fails Golem95 is called as a rescue system. On the right branch the call to SAMURAI is skipped and Golem95 is used as the sole tensor reduction method.

3 Applications

3.1 Automated One-Loop Matrix Element Evaluation

We have combined the components described in Section 2 to build an automated general one-loop evaluator for matrix elements (GOLEM). The implementation is realised in form of a `python` program called `golem-2.0` [39–41]. We have recently added an interface for importing Feynman rules from FeynRules [42]. Furthermore, the program supports the Binoth Les Houches Accord [13] which defines a standard way of communicating information between Monte Carlo generators and one-loop matrix element codes. The numerical code is generated in `Fortran 95` using the optimising code generator `haggies` [43] but can be linked both by the `Fortran` [44] and `C` conventions.

3.2 Results for $pp \rightarrow b\bar{b}b\bar{b} + X$

At the LHC the signature of four b -jets can be a significant background for Higgs searches in models beyond the Standard Model [23,45,46]. Owing to large uncertainties and huge backgrounds this search channel has been neglected in most phenomenological studies for the LHC. Since in some BSM scenarios one of the Higgs bosons can be predominantly decay into a four- b final state, it will be crucial to include the NLO corrections in α_s in future studies.

In our setup, the virtual matrix elements have been generated using `golem-2.0` for the processes $q\bar{q}/gg \rightarrow q_1\bar{q}_1q_2\bar{q}_2$, where q , q_1 and q_2 represent different quark flavours. The amplitudes for the $b\bar{b}b\bar{b}$ final state have been obtained using the relation [40]

$$\mathcal{A}_{b\bar{b}b\bar{b}}(1, 2; 3, 4, 5, 6) = \mathcal{A}_{q_1\bar{q}_1q_2\bar{q}_2}(1, 2; 3, 4, 5, 6) - \mathcal{A}_{q_1\bar{q}_1q_2\bar{q}_2}(1, 2; 3, 6, 5, 4), \quad (9)$$

where a permutation of the momenta encodes a simultaneous permutation of momenta, colour and helicity labels. This trick reduces the number of diagrams and therefore the code size by a factor two. The Born level amplitude and the real emission corrections were calculated using `MadGraph` [47] and `MadEvent` [48]; for the subtraction of the infrared singularities `MadDipole` [8, 10] has been employed. On top of the programs described in Section 2, the library `OneLoop` [49] was used for the evaluation of the scalar integrals. The virtual corrections were integrated over phase space by reweighting sets of unweighted Born level events $\{p_i\}$. In order to obtain the virtual corrections for an observable defined by the measurement function $\mathcal{F}(\{p_i\})$ we evaluate the Monte Carlo sum

$$\langle \mathcal{F} \rangle_{\text{virt}} = \frac{\sigma_{\text{Born}}}{N} \sum_{i=1}^N \left(1 + \frac{\mathcal{A}_{\text{Born}}^\dagger \mathcal{A}_{\text{virt}} + h.c.}{\mathcal{A}_{\text{Born}}^\dagger \mathcal{A}_{\text{Born}}} \right) \mathcal{F}(\{p_i\}). \quad (10)$$

In order to obtain an estimate for the computational cost and the numerical stability of the generated code, we have evaluated the matrix element for 500 points, starting from a fixed kinematics as specified in [50] and rotating the final state particles about the z -axis which coincides with the direction of the incoming particles.

The results for the gluon induced subprocess are shown in Figure 2. As expected [50, 51] the amplitude develops a relatively sharp peak around $\theta_0 \approx 2.32$ and at $\theta_1 = \theta_0 + \pi$ because these points are close to a double parton scattering kinematics. On a Xeon 5500 CPU the computation of a single phase space point in our setup requires 18 seconds for the virtual corrections and 11 ms for the real corrections including subtractions.

4 Conclusion

In this talk we have reported on the status and various developments in the Golem and the SAMURAI project. SAMURAI is a program for the unitarity based reduction of one-loop amplitudes which, amongst other improvements, preserves the n -dimensional

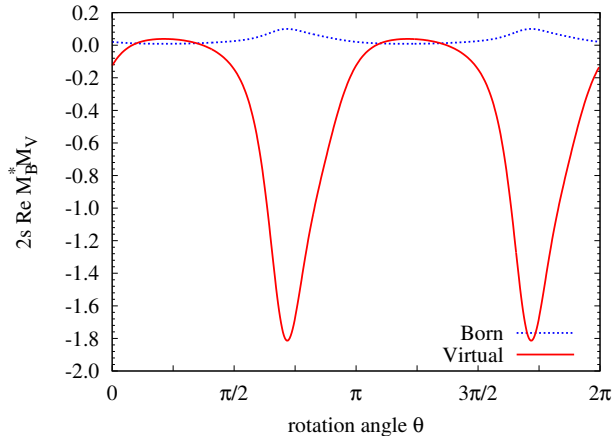


Figure 2: Born (dashed) matrix element squared and the interference term between Born and virtual corrections (straight line) of the $gg \rightarrow b\bar{b}b\bar{b}$ amplitude. The curves have been obtained by rotating the final state particles about the z -axis. The amplitude peaks around $\theta_0 \approx 2.32$ and $\theta_1 = \theta_0 + \pi$ which are points close to double parton scattering kinematics.

information of the numerator and is therefore capable of evaluating the amplitude including all rational terms. The tensor reduction library Golem95 has been extended with integrals with massive loop propagators; a new version extending the integrals further to the case of complex masses will be released soon. We have presented a method for the numerical reconstruction of tensor coefficients from the numerator of the integrand of a one-loop Feynman diagram, which can be used to combine the advantages of unitarity based and conventional tensor reduction methods. These different tensor reduction strategies are combined in the one-loop matrix element generator `golem-2.0`, which has been used for the calculation of the QCD corrections of the process $pp \rightarrow b\bar{b}b\bar{b} + X$. Phenomenological results for this process are to be expected soon.

References

- [1] S. Catani and M. Seymour, Nucl.Phys. **B485**, 291 (1997), arXiv:hep-ph/9605323.
- [2] S. Catani, S. Dittmaier, M. H. Seymour, and Z. Trocsanyi, Nucl.Phys. **B627**, 189 (2002), arXiv:hep-ph/0201036.
- [3] S. Frixione, Z. Kunszt, and A. Signer, Nucl.Phys. **B467**, 399 (1996), arXiv:hep-ph/9512328.
- [4] S. Frixione, Nucl.Phys. **B507**, 295 (1997), arXiv:hep-ph/9706545.

- [5] T. Gleisberg and F. Krauss, *Eur.Phys.J.* **C53**, 501 (2008), arXiv:0709.2881.
- [6] M. H. Seymour and C. Tevlin, (2008), arXiv:0803.2231.
- [7] K. Hasegawa, S. Moch, and P. Uwer, *Comput.Phys.Commun.* **181**, 1802 (2010), arXiv:0911.4371.
- [8] R. Frederix, T. Gehrmann, and N. Greiner, *JHEP* **0809**, 122 (2008), arXiv:0808.2128.
- [9] R. Frederix, S. Frixione, F. Maltoni, and T. Stelzer, *JHEP* **0910**, 003 (2009), arXiv:0908.4272.
- [10] R. Frederix, T. Gehrmann, and N. Greiner, *JHEP* **1006**, 086 (2010), arXiv:1004.2905.
- [11] T. Gehrmann and N. Greiner, (2010), arXiv:1011.0321.
- [12] M. Czakon, C. Papadopoulos, and M. Worek, *JHEP* **0908**, 085 (2009), arXiv:0905.0883.
- [13] T. Binoth *et al.*, *Comput.Phys.Commun.* **181**, 1612 (2010), arXiv:1001.1307, Dedicated to the memory of, and in tribute to, Thomas Binoth, who led the effort to develop this proposal for Les Houches 2009.
- [14] A. Bredenstein, A. Denner, S. Dittmaier, and S. Pozzorini, *JHEP* **0808**, 108 (2008), arXiv:0807.1248.
- [15] A. Bredenstein, A. Denner, S. Dittmaier, and S. Pozzorini, *Phys.Rev.Lett.* **103**, 012002 (2009), arXiv:0905.0110.
- [16] G. Bevilacqua, M. Czakon, C. Papadopoulos, R. Pittau, and M. Worek, *JHEP* **0909**, 109 (2009), arXiv:0907.4723.
- [17] R. Ellis, K. Melnikov, and G. Zanderighi, *Phys.Rev.* **D80**, 094002 (2009), arXiv:0906.1445.
- [18] C. Berger *et al.*, *Phys.Rev.* **D80**, 074036 (2009), arXiv:0907.1984.
- [19] C. Berger *et al.*, *Phys.Rev.* **D82**, 074002 (2010), arXiv:1004.1659.
- [20] C. Berger *et al.*, (2010), arXiv:1009.2338.
- [21] T. Melia, K. Melnikov, R. Rontsch, and G. Zanderighi, (2010), arXiv:1007.5313.
- [22] T. Binoth *et al.*, *Phys.Lett.* **B685**, 293 (2010), arXiv:0910.4379.

- [23] SM and NLO Multileg Working Group, J. Andersen *et al.*, (2010), arXiv:1003.1241.
- [24] P. Nogueira, J.Comput.Phys. **105**, 279 (1993).
- [25] J. Vermaseren, (2000), arXiv:math-ph/0010025.
- [26] G. Cullen, M. Koch-Janusz, and T. Reiter, (2010), arXiv:1008.0803.
- [27] G. Ossola, C. G. Papadopoulos, and R. Pittau, Nucl.Phys. **B763**, 147 (2007), arXiv:hep-ph/0609007.
- [28] G. Ossola, C. G. Papadopoulos, and R. Pittau, JHEP **0707**, 085 (2007), arXiv:0704.1271.
- [29] R. Ellis, W. Giele, and Z. Kunszt, JHEP **0803**, 003 (2008), arXiv:0708.2398.
- [30] W. T. Giele, Z. Kunszt, and K. Melnikov, JHEP **0804**, 049 (2008), arXiv:0801.2237.
- [31] K. Melnikov and M. Schulze, Nucl.Phys. **B840**, 129 (2010), arXiv:1004.3284.
- [32] P. Mastrolia, G. Ossola, T. Reiter, and F. Tramontano, JHEP **1008**, 080 (2010), arXiv:1006.0710.
- [33] A. Denner and S. Dittmaier, Nucl.Phys. **B734**, 62 (2006), arXiv:hep-ph/0509141.
- [34] T. Binoth, J. Guillet, and G. Heinrich, Nucl.Phys. **B572**, 361 (2000), arXiv:hep-ph/9911342.
- [35] T. Binoth, J. Guillet, G. Heinrich, E. Pilon, and C. Schubert, JHEP **0510**, 015 (2005), arXiv:hep-ph/0504267.
- [36] T. Binoth, J. Guillet, and G. Heinrich, JHEP **0702**, 013 (2007), arXiv:hep-ph/0609054.
- [37] T. Binoth, J.-P. Guillet, G. Heinrich, E. Pilon, and T. Reiter, Comput.Phys.Commun. **180**, 2317 (2009), arXiv:0810.0992.
- [38] G. Heinrich, G. Ossola, T. Reiter, and F. Tramontano, JHEP **1010**, 105 (2010), arXiv:1008.2441.
- [39] T. Binoth *et al.*, Nucl.Phys.Proc.Suppl. **183**, 91 (2008), arXiv:0807.0605.
- [40] T. Reiter, (2009), arXiv:0903.0947.
- [41] T. Reiter, (2009), arXiv:0903.4648.

- [42] N. D. Christensen and C. Duhr, *Comput.Phys.Commun.* **180**, 1614 (2009), arXiv:0806.4194.
- [43] T. Reiter, *Comput.Phys.Commun.* **181**, 1301 (2010), arXiv:0907.3714.
- [44] ISO/IEC JTC1/SC22, ISO/IEC Report No. 1539-1:2004, 2003.
- [45] R. Lafaye, . Miller, D.J., M. Muhlleitner, and S. Moretti, (2000), arXiv:hep-ph/0002238.
- [46] W. Krolkowski, (2008), arXiv:0803.2977.
- [47] T. Stelzer and W. Long, *Comput.Phys.Commun.* **81**, 357 (1994), arXiv:hep-ph/9401258.
- [48] F. Maltoni and T. Stelzer, *JHEP* **0302**, 027 (2003), arXiv:hep-ph/0208156.
- [49] A. van Hameren, (2010), arXiv:1007.4716.
- [50] W. Gong, Z. Nagy, and D. E. Soper, *Phys.Rev.* **D79**, 033005 (2009), arXiv:0812.3686.
- [51] C. Bernicot and J.-P. Guillet, *JHEP* **0801**, 059 (2008), arXiv:0711.4713.